Organometallic Isocyanocyclopentadienides: A Combined Synthetic, Spectroscopic, Structural, Electrochemical, and Theoretical Investigation

Thomas C. Holovics,† Stephan F. Deplazes,† Masaharu Toriyama,‡ Douglas R. Powell,† Gerald H. Lushington,† and Mikhail V. Barybin*,†

Department of Chemistry, University of Kansas, 1251 Wescoe Hall Drive, Lawrence, Kansas 66045, and College of Pharmacy, Nihon University, 7-7-1 Narashinodai, Funabashi-shi, Chiba 274-8555, Japan

Received March 2, 2004

This article reports on the chemistry of two organometallic isocyanocyclopentadienides, which represent an emerging new class of aromatic isocyanides incorporating nonbenzenoid π-systems. Interaction of aminoferrocene with a mixture of phenyl formate/phenol followed by subsequent dehydration of the resulting ferrocenylformamide with $POCl_3$ produced air and thermally stable isocyanoferrocene (CNFc, Fc = ferrocenyl) in a high yield. Treating lithiocymantrene, LiCm (Cm = $(\eta^5\text{-}C_5H_4)Mn(CO)_3$), with tosyl azide afforded thermally sensitive cymantrenyl azide. Without isolation, CmN_3 was reduced by $NaBH_4$ to form aminocymantrene, which was converted into air stable but thermally and light sensitive isocyanocymantrene, CNCm. Combining 6 equiv of CNR (R = Fc, Cm) with bis(naphthalene)-chromium(0) afforded $Cr(CNR)_6$. Successive one-electron oxidations of $Cr(CNR)_6$ with Ag^+ produced the corresponding paramagnetic $[Cr(CNR)_6]^+$ and $[Cr(CNR)_6]^{2+}$. The compounds $[Cr(CNR)_6]^{0,1+,2+}$ (R = Fc, Cm) are remarkable due to the incorporation of seven transition metal atoms within relatively compact ML_6 motifs. The physical, chemical, electrochemical, and spectroscopic properties of the structurally characterized series $[Cr(CNFc)_6]^{0,1+,2+}$ indicate that the electronic influence of the ferrocenyl moiety, often compared to an alkyl group, is in fact more similar to that of aryl substituents. Electrochemical properties of $[Cr(CNR)_6]^{0,1+,2+}$ (R = Fc, Cm) are consistent with isocyanocymantrene being a substantially stronger π-acid than isocyanoferrocene. This conclusion was unambiguously corroborated by a DFT analysis of the Frontier molecular orbitals of CNFc and CNCm. Unpaired spin delocalization within odd-atom, nonbenzenoid aromatic π-systems of $[Cr(CNR)_6]^{1+,2+}$ (R = Fc, Cm) was studied by multinuclear paramagnetic NMR and contrasted with patterns observed for similar complexes incorporating benzenoid and even-atom, nonbenzenoid aromatic moieties.

Introduction

Organic isocyanides (:C≡N−R), also referred to as isonitriles or carbylamines, are among the few isolable species possessing a lone electron pair on a carbon atom. The most general route to these highly reactive substances involves formylation of the corresponding primary amine, H_2NR, followed by dehydration of the resulting formamide, H(O)CNHR.[1] Given the important role of isocyanides in organic and organometallic synthesis,[1,2] catalysis,[2a−c] materials science,[3] drug discovery,[4] and diagnostic medicine,[5] it is surprising that the extensive work in these areas continues to rely on a fundamentally quite limited pool of isocyanide molecules.[1−5] Aryl isocyanides, CNAr, are generally more thermally and air sensitive than alkyl isocyanide congeners thereof.[6] For instance, CNPh and a number of its derivatives deteriorate rapidly upon exposure to air and isomerize to the corresponding thermodynamically favored cyanides at 40−50 °C.[7]

The electronic advantage of aryl over alkyl isocyanides stems from communication between the π-systems of the isocyano group and the aromatic moiety within the former species.[2,8] Isocyanoferrocene[9] and 1,1′-diisocyanoferrocene,[10] which may be regarded as organometallic derivatives of the elusive[11] isocyanocyclopentadienide anion, were the only known examples of *non-*

* To whom correspondence should be addressed. E-mail: mbarybin@ku.edu.
† University of Kansas.
‡ Nihon University.

(1) Ugi, I. *Isonitrile Chemistry*; Academic Press: New York, 1971.
(2) (a) Singleton, E.; Oosthuizen, H. E. *Adv. Organomet. Chem.* **1983**, *22*, 209−309. (b) Treichel, P. M. *Adv. Organomet. Chem.* **1973**, *11*, 21−86. (c) Yamamoto, Y. *Coord. Chem. Rev.* **1980**, *32*, 193−233. (d) Carnahan, E. M.; Protasiewicz, J. D.; Lippard, S. J. *Acc. Chem. Res.* **1993**, *26*, 90−97. (e) Weber, L. *Angew. Chem., Int. Ed.* **1998**, *37*, 1515−1517. (f) Hahn, F. E. *Angew. Chem., Int. Ed. Engl.* **1993**, *32*, 650−665.
(3) (a) Cornelissen, J. L. M.; Rowan, A. E.; Nolte, R. J. M.; Sommerdijk, N. A. J. M. *Chem. Rev.* **2001**, *101*, 4039−4070. (b) Nakano, T.; Okamoto, Y. *Chem. Rev.* **2001**, *101*, 4013−4038.
(4) (a) Ugi, I.; Werner, B.; Dömling, A. *Molecules* **2003**, *8*, 53−66. (b) Weber, L. *Curr. Med. Chem.* **2002**, *9*, 1241−1253. (c) Dömling, A. *Curr. Opin. Chem. Biol.* **2002**, *6*, 306−313. (d) Ugi, I. *Pure Appl. Chem.* **2001**, *73*, 187−191. (e) Dömling, A. *Curr. Opin. Chem. Biol.* **2000**, *6*, 318−323.
(5) Sharma, V.; Piwnica-Worms, D. *Chem. Rev.* **1999**, *99*, 2545−2560.
(6) Malatesta, L. *Prog. Inorg. Chem.* **1959**, *1*, 283−379.
(7) Meier, M.; Mueller, B.; Ruechardt, C. *J. Org. Chem.* **1987**, *52*, 648−652.

10.1021/om049842n CCC: $27.50
Publication on Web 05/13/2004

benzenoid aryl isocyanides prior to our recent communications.[12,13] The chemistry of isocyanoferrocene has remained practically unexplored since discovery of the compound in the late 1980s.[9] This may be attributed to the fact that only tedious and very low-yield (8−12% starting from ferrocene) syntheses of aminoferrocene were available until recently.[14] Furthermore, conversion of H_2NFc to CNFc (Fc = ferrocenyl) has been reported to be poorly reproducible.[9a] The isolated complexes of CNFc have been limited to $(OC)_5Cr(CNFc)$ and $(OC)_4Fe(CNFc)$.[9] Notably, the electronic properties of isocyanoferrocene as a ligand have been suggested to be similar to those of methyl isocyanide on the basis of electrochemical characteristics of $(OC)_5Cr(CNR)$ (R = Fc, Me) and the long-accepted fact[15] that ferrocenyl is a slightly stronger electron-donating substituent than methyl.[9b,c] Despite many parallels in the chemistries of ferrocene and arenes, consideration of ferrocenyl's π-system as a potential electron acceptor has not been addressed experimentally. This is not surprising given that the five-membered rings of Cp_2Fe already possess an effective negative charge of ca. 0.35.[15]

The traditional methods of tuning properties of aryl isocyanides have revolved around the π-system of benzene for decades and are based on C−H substitution at the aromatic ring.[1,2,6,8] Altering the nature of the metal fragment in η^5-bound isocyanocyclopentadienyl complexes would constitute a fundamentally new approach for modulating electronic and structural characteristics of aromatic isocyanides. Herein, we report on the efficient synthesis and properties of isocyanoferrocene and of the hitherto unknown isocyanocymantrene, CNCm {Cm = cymantrenyl or $(\eta^5\text{-}C_5H_4)Mn(CO)_3$}. Heptanuclear, binary complexes of these organometallic isocyanocyclopentadienides, namely, $[Cr(CNR)_6]^{0,1+,2+}$ (R = Fc, Cm), are described as well. A preliminary account of a portion of this work has been communicated.[12]

Experimental Section

General Procedures, Starting Materials, and Equipment. Unless specified otherwise, all operations were performed under an atmosphere of 99.5% argon purified by passage through columns of activated BASF catalyst and molecular sieves. All connections involving the gas purification system were made of glass, metal, or other materials impermeable to air. Solutions were transferred via stainless steel needles (cannulas) whenever possible. Standard Schlenk techniques were employed with a double manifold vacuum line. Solvents, including deuterated solvents, were freed of impurities by standard procedures and stored under argon.

Solution infrared spectra were recorded on a Thermo Nicolet Avatar 360 FTIR spectrometer with samples sealed in 0.1 mm gastight NaCl cells. NMR samples were analyzed on Bruker DRX-400 or Bruker Avance 500 spectrometers. ^1H and ^{13}C chemical shifts are given with reference to residual ^1H and ^{13}C solvent resonances relative to $SiMe_4$. Such referencing eliminated bulk susceptibility effects for paramagnetic samples. Two-dimensional NMR techniques (DQF-COSY, $^1H-^{13}C$ HMQC, and $^1H-^{13}C$ HMBC)[16] were employed to obtain unambiguous assignments of ^1H and ^{13}C NMR resonances. The aromatic hydrogen resonances are labeled in reference to the corresponding carbon atoms. ^{14}N NMR chemical shifts are referenced to liquid NH_3 at 25 °C. In the variable-temperature NMR studies, the console temperature was calibrated using a thermocouple immersed into an NMR tube containing pure solvent (CD_2Cl_2). Melting points are uncorrected and were determined for samples in sealed capillary tubes. Elemental analyses were carried out by Desert Analytics, Tucson, AZ.

Phenyl formate,[17] acetic-formic anhydride,[18] $V(CO)_6$,[19] $[Et_4N][V(CO)_6]$,[20] tosyl azide,[21] bis(η^6-naphthalene)chromium(0),[22] and aminoferrocene[14b] were prepared according to literature procedures. Other reagents were obtained from commercial sources and freed of oxygen and moisture before use, if required.

Magnetic Susceptibility Measurements. Solid-state volume magnetic susceptibilities were measured on a Johnson Matthey MSB-1 balance at ambient temperature and converted into the corresponding molar susceptibilities in the usual manner.[23] Samples were packed into gastight tubes (0.400 cm o.d. × 0.324 cm i.d.) to a depth of ca. 3 cm in a drybox. The air correction of 0.029×10^{-6} was applied to volume susceptibilities of all samples packed under argon. Diamagnetic corrections applied to the molar susceptibilities of the paramagnetic substances are reported as χ_{diam}. These corrections were obtained by adding contributions from the $[BF_4]^-$ or $[SbF_6]^-$ ions[23] to experimentally determined molar susceptibilities of diamagnetic $Cr(CNFc)_6$ or $Cr(CNCm)_6$. The molar susceptibilities of $Cr(CNFc)_6$ and $Cr(CNCm)_6$ at 25 °C were *measured* to be -403.4×10^{-6} and -300.2×10^{-6} cm^3 mol^{-1}, respectively.

Synthesis of FcNHC(O)H (1). Approximately 3 mL of a 65/35 mol % mixture of phenyl formate/phenol[17] was added to solid $FcNH_2$ (0.958 g, 4.77 mmol) in one portion at room

(8) Selected examples: (a) Chen, J.; Calvet, L. C.; Reed, M. A.; Carr, D. W.; Grubisha, D. S.; Bennett, D. W. *Chem. Phys. Lett.* **1999**, *313*, 741−748. (b) Wagner, N. L.; Laib, F. E.; Bennett, D. W. *Inorg. Chem. Commun.* **2000**, *3*, 87−90. (c) Henderson, J. I.; Feng, S.; Bein, T.; Kubiak, C. P. *Langmuir* **2000**, *16*, 6183−6187. (d) Hanack, M.; Kamenzin, S.; Kamenzin, C.; Subramanian, L. *Synth. Met.* **2000**, *110*, 93−102.

(9) (a) Knox, G. R.; Pauson, P. L.; Willison, D.; Solcániová, E.; Toma. *Organometallics* **1990**, *9*, 301−306. (b) El-Shihi, T.; Siglmüller, F.; Herrmann, R.; Carvalho, M. F. N. N.; Pombeiro, A. J. L. *J. Organomet. Chem.* **1987**, *335*, 239−247. (c) El-Shihi, T.; Siglmüller, F.; Herrmann, R.; Carvalho, M. F. N. N.; Pombeiro, A. J. L. *Port. Electrochim. Acta* **1987**, *5*, 179−185.

(10) Van Leusen, D.; Hessen, B. *Organometallics* **2001**, *20*, 224−226.

(11) Banert, K.; Köehler, F.; Meier, B. *Tetrahedron Lett.* **2003**, *44*, 3781−3783.

(12) Barybin, M. V.; Holovics, T. C.; Deplazes, S. F.; Lushington, G. H.; Powell, D. R.; Toriyama, M. *J. Am. Chem. Soc.* **2002**, *124*, 13668−13669.

(13) Robinson, R. E.; Holovics, T. C.; Deplazes, S. F.; Lushington, G. H.; Powell, D. R.; Barybin, M. V. *J. Am. Chem. Soc.* **2003**, *125*, 4432−4433.

(14) Improved syntheses of aminoferrocene and 1,1′-diaminoferrocene have recently been published: (a) ref 10. (b) Bildstein, B.; Malaun, M.; Kopacka, H.; Wurst, K.; Mitterböck, M.; Ongania, K.-H.; Opromolla, G.; Zanello, P. *Organometallics* **1999**, *18*, 4325−4336. (c) Kavallieratos, K.; Hwang, S.; Crabtree, R. H. *Inorg. Chem.* **1999**, *38*, 5184−5186. (d) Shafir, A.; Power, M. P.; Whitener, G. D.; Arnold, J. *Organometallics* **2000**, *19*, 3978−3982.

(15) Nesmeyanov, A. N.; Perevalova, E. G.; Gibin, S. P.; Grandberg, K. I.; Kozlovsky, A. G. *Tetrahedron Lett.* **1966**, *22*, 23−81−2387.

(16) Levitt, M. H. *Spin Dynamics. Basics of Nuclear Magnetic Resonance*; John Wiley & Sons, Ltd: New York, 2001.

(17) Yale, H. L. *J. Org. Chem.* **1971**, *36*, 3228−3240.

(18) Krimen, L. I. *Org. Synth.* **1970**, *50*, 1−3.

(19) (a) Liu, X.; Ellis, J. E. *Inorg. Synth.* **2004**, *34*, 96−103. (b) Ellis, J. E.; Faltynek, R. A.; Rochfort, G. L.; Stevens, R. E.; Zank, G. A. *Inorg. Chem.* **1980**, *19*, 1082−1085.

(20) Barybin, M. V.; Pomije, M. K.; Ellis, J. E. *Inorg. Chim. Acta* **1998**, *269*, 58−62.

(21) Regitz, M.; Hocker, J. *Organic Syntheses*; John Wiley: New York, 1973; Collect. Vol. V, pp 179−183.

(22) (a) Pomije, M. K.; Kurth, C. J.; Ellis, J. E.; Barybin, M. V. *Organometallics* **1997**, *16*, 3582−3587. (b) Kündig, E. P.; Timms, P. L. *J. Chem. Soc., Dalton. Trans.* **1980**, 991−995.

(23) (a) Earnshaw, A. *Introduction to Magnetochemistry*; Academic Press: New York, 1968. (b) Kahn, O. *Molecular Magnetism*; VCH Publishers: New York, 1993.

temperature under argon with vigorous stirring. A slightly exothermic reaction occurred, affording a brown solution within a minute. After 4 h of stirring at room temperature, complete consumption of $FcNH_2$ was confirmed by TLC using neat Et_2O as eluent. All volatiles were removed under vacuum (5×10^{-3} Torr) at $T < 50$ °C (important!) using short-path distillation equipment. The residual oil was dissolved in Et_2O and passed through a 30 cm column packed with Florisil. An intensely orange solution was collected. All Et_2O was removed, leaving an orange oil, which was recrystallized from Et_2O, providing a 79% yield of crystalline orange **1** (0.860 g, 3.75 mmol), which was spectroscopically (IR, ^1H and ^{13}C NMR) identical to *bona fide* ferrocenylformamide.[9a] Mp: 92−94 °C (lit. 86−87 °C[9a]).

Synthesis of CNFc (2). This procedure is highly reliable and constitutes a modified version of the poorly reproducible synthesis reported by Knox et al.[9a] Phosphorus oxychloride (0.915 mL, 9.78 mmol) was added at once to a stirred solution of **1** (2.222 g, 9.70 mmol) and freshly distilled $^iPr_2NH$ (4.08 mL, 29.1 mmol) in 50 mL of CH_2Cl_2 at ambient temperature. After stirring for 10 h, the reaction mixture was quenched with 100 mL of 10% aqueous potassium carbonate. The organic layer was separated, washed with distilled water (2×50 mL), and dried over $MgSO_4$ without protection from air. Filtration of the resulting orange solution followed by solvent removal afforded crude CNFc as an orange solid. This solid was dissolved in hexanes and passed through a 25 cm column of Florisil using a 1:1 mixture of hexanes/Et_2O. The solvent was removed in vacuo to provide a 93% yield of spectroscopically pure, microcrystalline, peach-colored **2** (1.907 g, 9.04 mmol). Mp = 73−75 °C (lit. 76−77 °C[9a]). IR (CH_2Cl_2): ν_{CN} 2122 vs cm^{-1}. ^1H NMR (400 MHz, $CDCl_3$, 25 °C): δ 4.13 (ψ-t, 2H, C_5H_4, $H^{3,4}$), 4.32 (s, 5H, C_5H_5), 4.57 (ψ-t, 2H, C_5H_4, $H^{2,5}$) ppm. $^{13}C\{^1H\}$ NMR (100.6 MHz, $CDCl_3$, 25 °C): δ 67.2 (C_5H_4, $C^{2,5}$), 67.2 (C_5H_4, $C^{3,4}$), 71.0 (C_5H_5), 174.0 (*C*NFc) ppm. ^{14}N NMR (36.2 MHz, $CDCl_3$, 25 °C): δ 172.1 ($W1/2 = 28$ Hz) ppm.

Synthesis of $CmNH_2$. A 1.60 M solution of ^{n}BuLi in hexanes (23.5 mL, 37.60 mmol) was added dropwise to a cold (−78 °C), pale yellow solution of cymantrene (7.680 g, 37.63 mmol) in 150 mL of THF. After 1 h of vigorous stirring at −78 °C, the yellow-orange reaction mixture was treated with a solution of *p*-toluenesulfonyl azide (7.424 g, 37.64 mmol) in 75 mL of THF. The resulting deep red-orange mixture was allowed to warm to room temperature for 13 h in the dark. Formation of cymantrenyl azide, CmN_3, was confirmed by FTIR (ν_{NN} 2129 m; ν_{CO} 2021 s, 1934 vs cm^{-1}). All solvent was subsequently removed in vacuo, and the oily residue was redissolved in ca. 150 mL of EtOH. To this solution $NaBH_4$ (7.424 g, 37.64 mmol) dissolved in 150 mL of EtOH was carefully added at room temperature. A vigorous exothermic reaction occurred. After the gas evolution had ceased, the orange mixture was extracted with Et_2O (300 mL). The ethereal layer was washed with 300 mL of H_2O and then treated with 300 mL of water acidified to pH = 3 with 1.0 M HCl. The aqueous layer was separated and neutralized to pH = 8 with 1.0 M NaOH. Extraction with Et_2O afforded an orange-yellow solution of $CmNH_2$, which was dried over Na_2SO_4, filtered, and concentrated to dryness to provide orange-yellow $CmNH_2$ (5.689 g, 25.97 mmol) in a 69% yield. Mp = 74−76 °C (lit. 77−77.5 °C[24]). IR (Et_2O): ν_{NH} 3460 w, 3386 w; ν_{CO} 2012 s, 1921 vs cm^{-1}. The product may contain a small amount of cymantrene and can be further purified by column chromatography or sublimation,[24] if desired. Such a purification, however, is not necessary for the synthesis of CmNHC(O)H.

Synthesis of CmNHC(O)H (3). *Crude* $CmNH_2$ (5.689 g, 25.97 mmol), obtained in the above synthesis, was dissolved in 30 mL of CH_2Cl_2 and treated dropwise with a solution of excess acetic-formic anhydride[18] (67.40 mmol) in 30 mL of CH_2Cl_2. After stirring for 20 min, the reaction mixture was washed sequentially with 200 mL of saturated aqueous Na_2CO_3 and 100 mL of H_2O, dried over sodium sulfate, concentrated, and chromatographed on silica gel. A trace amount of cymantrene was eluted with hexanes, while the subsequent elution with Et_2O provided a yellow solution of **3**. Solvent removal followed by drying under vacuum for 2 h afforded analytically pure, bright yellow **3** (5.100 g, 20.64 mmol) in an 80% yield (or a 55% *overall* yield based on the starting amount of cymantrene used in the above synthesis of $CmNH_2$). Mp: 97−100 °C dec. Anal. Calcd for $C_9H_6NMnO_4$: C, 43.75; H, 2.45; N, 5.67. Found: C, 44.06; H, 2.52; N, 5.71. IR (CH_2Cl_2): ν_{NH} 3415 w; ν_{CO} 2022 s, 1935 vs, 1706 m cm^{-1}. In dichloromethane solutions at 25 °C, **3** exists as a 9:1 mixture of two conformational isomers. The following NMR data refer to the major isomer. ^1H NMR (500 MHz, CD_2Cl_2, 25 °C): δ 4.64 (s, 2H, C_5H_4, $H^{3,4}$), 5.13 (s, 2H, C_5H_4, $H^{2,5}$), 7.33 (s, 1H, N*H*). 8.20 (s, 1H, *formyl H*) ppm. $^{13}C\{^1H\}$ NMR (125.8 MHz, CD_2Cl_2, 25 °C): δ 73.4 (C_5H_4, $C^{2,5}$), 79.6 (C_5H_4, $C^{3,4}$), 111.1 (C_5H_4, C^1), 159.6 (*formyl C*), 225.4 (Mn{*CO*}$_3$) ppm.

Synthesis of CNCm (4). Phosphorus oxychloride (0.91 mL, 9.73 mmol) was added at once to a stirred yellow solution of **2** (2.000 g, 8.09 mmol) and Et_3N (5.60 mL, 40.2 mmol) in 150 mL of CH_2Cl_2 at ambient temperature. After stirring for 1 h, the reaction was quenched with 300 mL of 10% aqueous sodium carbonate. The organic layer was separated, washed with distilled water (2×150 mL), and dried over Na_2SO_4 without protection from air. The yellow solution was filtered and evaporated to dryness under reduced pressure. The residue was passed through a 20 cm column of Florisil using a 1:1 mixture of hexanes/CH_2Cl_2 to elute a fast moving yellow band. The solvent was removed in vacuo (5×10^{-3} Torr) at 0 °C (*important!*) to afford tan-yellow **4** in an 81% yield (1.500 g, 6.55 mmol). Mp = 26−29 °C dec. IR (CH_2Cl_2): ν_{CN} 2133 m; ν_{CO} 2034 s 1952 vs cm^{-1}. ^1H NMR (500 MHz, CD_2Cl_2, 25 °C): δ 4.66 (s, 2H, C_5H_4, $H^{3,4}$), 5.11 (s, 2H, C_5H_4, $H^{2,5}$) ppm. $^{13}C\{^1H\}$ NMR (125.8 MHz, CD_2Cl_2, 25 °C): δ 80.7 (C_5H_4, $C^{3,4}$), 81.7 (C_5H_4, $C^{2,5}$), 91.8 (C_5H_4, C^1), 168.9 (*C*NCm), 223.6 (*C*O) ppm. ^{14}N NMR (36.2 MHz, $CDCl_3$, 25 °C): δ 164.3 ($W1/2 = 41$ Hz) ppm. Elemental analysis of **4** was not sought due to the poor stability of its samples at ambient temperature.

Synthesis of $Cr(CNFc)_6$ (5). An orange solution of **2** (1.900 g, 9.00 mmol) in 50 mL of THF was added to a brown solution of bis(η^6-naphthalene)chromium(0) (0.427 g, 1.39 mmol) in 70 mL of THF via cannula at room temperature. Within 15 h of stirring, a deep orange-red solution/slurry formed. Heptane (20 mL) was introduced to the reaction mixture, and all but about 40 mL of the solvent was removed under vacuum. The precipitate was filtered off and washed thoroughly with pentane (4×15 mL) to remove naphthalene and any unreacted **2**. After drying in vacuo for 3 h, microcrystalline, orange-red **5** (1.696 g, 1.29 mmol) was isolated in a 93% yield. Mp: 256−257 °C dec. Anal. Calcd for $C_{66}H_{54}N_6CrFe_6$: C, 60.13; H, 4.13; N, 6.38. Found: C, 60.22; H, 3.89; N, 6.18. $[M + 1]^+$ Calcd for $C_{66}H_{54}N_6{}^{52}Cr^{56}Fe_6$: 1320.2. Found: 1320.5. IR (CH_2Cl_2): ν_{CN} 1971 vs br cm^{-1}. ^1H NMR (400 MHz, CD_2Cl_2, 25 °C): δ 4.18 (s, 2H, C_5H_4, $H^{3,4}$), 4.27 (s, 2H, C_5H_4, $H^{2,5}$), 4.34 (s, 5H, C_5H_5) ppm. $^{13}C\{^1H\}$ NMR (100.6 MHz, CD_2Cl_2, 25 °C): δ 67.6 (C_5H_4, $C^{2,5}$), 67.6 (C_5H_4, $C^{3,4}$), 70.8 (C_5H_5) ppm. ^{14}N NMR (36.2 MHz, CD_2Cl_2, 25 °C): δ 310.4 ($W1/2 = 77$ Hz) ppm.

Synthesis of $Cr(CNCm)_6$ (6). A yellow solution of **4** (1.500 g, 6.55 mmol) in 60 mL of THF was added to a brown solution of bis(η^6-naphthalene)chromium(0) (0.330 g, 1.07 mmol) in 60 mL of THF via cannula at −78 °C with vigorous stirring. The reaction mixture was allowed to warm gradually to room temperature. Within 15 h of stirring, a deep red solution formed. All but ca. 10 mL of the solvent was removed under vacuum, and 50 mL of heptane was added to precipitate a microcrystalline, red solid. An additional 10 mL of the solvent was removed, and 50 mL of pentane was added to the mixture. The precipitate was filtered off and washed thoroughly with

(24) Cais, M.; Narkis, N. *J. Organomet. Chem.* **1965**, *3*, 188−199.

pentane (4 × 15 mL) to remove naphthalene and any unreacted free ligand. After drying in vacuo for 3 h, microcrystalline, scarlet **6** (1.390 g, 0.974 mmol) was isolated in a 91% yield. Mp: 118−120 °C dec. Anal. Calcd for $C_{54}H_{24}N_6CrMn_6O_{18}$: C, 45.47; H, 1.70; N, 5.89. Found: C, 45.12; H, 1.70; N, 5.65. IR (CH_2Cl_2): ν_{CN} 1947 m br; ν_{CO} 2030 s, 1937 vs cm^{-1}. ^{1}H NMR (500 MHz, CD_2Cl_2, 25 °C): δ 4.63 (s, 2H, C_5H_4, $H^{3,4}$), 4.87 (s, 2H, C_5H_4, $H^{2,5}$), ppm. ^{13}C{^{1}H} NMR (125.8 MHz, CD_2Cl_2, 25 °C): δ 78.7 (C_5H_4, $C^{2,5}$), 80.2 (C_5H_4, $C^{3,4}$), 101.4 (C_5H_4, C^1), 224.9 (*C*O) ppm. ^{14}N NMR (36.2 MHz, CD_2Cl_2, 25 °C): δ 169.1 ($W1/2$ = 1115 Hz) ppm.

Synthesis of [Cr(CNFc)$_6$][BF$_4$] (5$^+$[BF$_4$]). A solution of **5** (0.980 g, 0.743 mmol) in 120 mL of CH_2Cl_2 was added to solid $AgBF_4$ (0.145 g, 0.745 mmol) at once with stirring at room temperature. The color of the reaction mixture changed from orange-red to orange-brown within minutes. The mixture was stirred for 6 h at ambient temperature, then filtered through a 3 cm plug of Celite. An additional 50 mL of CH_2Cl_2 was employed to wash the filter cake until the washings were colorless. All but ca. 35 mL of the solvent was removed under vacuum, and 35 mL of heptane was added to precipitate a microcrystalline, saddle-brown solid. This solid was filtered off, washed with pentane (2 × 20 mL), and dried in vacuo for 2 h to afford saddle-brown **5**$^+$[BF_4] (1.020 g, 0.726 mmol) in a 98% yield. Mp: 205 °C dec. Anal. Calcd for $C_{66}H_{54}N_6BCrF_4Fe_6$: C, 56.42; H, 3.87; N, 5.98. Found: C, 56.00; H, 3.86; N, 5.53. IR (CH_2Cl_2): ν_{CN} 2053 vs; ν_{BF} 1065 m br cm^{-1}. ^{1}H NMR (400 MHz, CD_2Cl_2, 25 °C): δ 1.32 (s, 2H, C_5H_4, $H^{2,5}$), 3.98 (s, 5H, C_5H_5), 5.73 (s, 2H, C_5H_4, $H^{3,4}$) ppm. ^{13}C{^{1}H} NMR (100.6 MHz, CD_2Cl_2, 25 °C): δ 71.7 (C_5H_5), 77.5 (C_5H_4, $C^{3,4}$), 109.2 (C_5H_4, $C^{2,5}$) ppm. ^{14}N NMR (36.2 MHz, CD_2Cl_2, 25 °C): δ 863.5 ($W1/2$ = 531 Hz) ppm. μ_{eff}(24.5 °C) = 1.78 μ_B (χ_{diam} = −442.4 × 10^{-6} cm^3 mol^{-1}).

Synthesis of [Cr(CNFc)$_6$][V(CO)$_6$] (5$^+$[V(CO)$_6$]). A yellow solution of $V(CO)_6$ (0.037 g, 0.169 mmol) in 30 mL of CH_2Cl_2 was added to an orange-red solution of **5** (0.220 g, 0.167 mmol) in 100 mL of CH_2Cl_2 with stirring at −55 °C. The reaction mixture acquired an orange-brown color within minutes. Upon warming to ambient temperature for 30 min, the mixture was filtered through a 3 cm plug of Celite. An additional 50 mL of CH_2Cl_2 was employed to wash the filter cake until the washings were colorless. After removing all but ca. 10 mL of the solvent under vacuum, 20 mL of heptane was added to the filtrate to precipitate a microcrystalline, brown solid. The product was filtered, washed with pentane (3 × 20 mL), and dried in vacuo to afford saddle-brown **5**$^+$[$V(CO)_6$] (0.242 g, 0.157 mmol) in a 94% yield. Compound **5**$^+$[$V(CO)_6$] decomposes at ca. 250 °C without melting. IR (CH_2Cl_2): ν_{CN} 2053 vs; ν_{CO} 1853 vs cm^{-1}. The ^{1}H and ^{13}C NMR (CD_2Cl_2, 25 °C) spectra for the cation in **5**$^+$[$V(CO)_6$]$^-$ were essentially identical to the corresponding patterns reported above for **5**$^+$[BF_4]$^-$.

Synthesis of [Cr(CNCm)$_6$][SbF$_6$] (6$^+$[SbF$_6$]). A colorless solution of $AgSbF_6$ (0.159 g, 0.463 mmol) in 60 mL of CH_2Cl_2 was added to a red solution of **6** (0.600 g, 0.421 mmol) in 60 mL of CH_2Cl_2 with vigorous stirring at room temperature. The reaction mixture turned dark green over a period of 1 h and then was filtered through a 3 cm plug of Celite. An additional 50 mL of CH_2Cl_2 was used to wash the filtercake until the washings were colorless. The filtrate was concentrated to ca. 10 mL under vacuum. Addition of heptane (40 mL) followed by removal of about 10 mL of the solvent produced a green precipitate. This solid was filtered, washed with pentane (3 × 15 mL), and dried in vacuo for 2 h to afford microcrystalline, lime-green **6**$^+$[SbF_6] (0.652 g, 0.392 mmol) in a 93% yield. Mp: 226−229 °C dec. Anal. Calcd for $C_{54}H_{24}N_6CrF_6Mn_6O_{18}Sb$: C, 39.02; H, 1.46; N, 5.06. Found: C, 38.83; H, 1.42; N, 4.68. IR (CH_2Cl_2): ν_{CN} 2073 m br; ν_{CO} 2029 s, 1950 vs; ν_{SbF} 596 s cm^{-1}. ^{1}H NMR (400 MHz, CD_2Cl_2, 22 °C): δ 0.17 (s, 2H, C_5H_4, $H^{2,5}$), 5.95 (s, 2H, C_5H_4, $H^{3,4}$), ppm. ^{13}C{^{1}H} NMR (100.6 MHz, CD_2Cl_2, 22 °C): δ 85.0 (C_5H_4, $C^{3,4}$), 145.0 (C_5H_4, $C^{2,5}$), 217.4 (*C*O) ppm. ^{14}N NMR (36.2 MHz, CD_2Cl_2, 22 °C): δ 866.2 ($W1/2$ = 1170 Hz) ppm. μ_{eff}(24.0 °C) = 1.99 μ_B (χ_{diam} = −380.2 × 10^{-6} cm^3 mol^{-1}).

Attempted Oxidation of 6 with V(CO)$_6$. A yellow solution of $V(CO)_6$ (0.051 g, 0.233 mmol) in 30 mL of CH_2Cl_2 was added to an orange-red solution of **6** (0.300 g, 0.210 mmol) in 100 mL of CH_2Cl_2 with stirring at −55 °C. The mixture was warmed to room temperature. Formation of only trace amounts of **6**$^+$[$V(CO)_6$] was observed by FTIR. However, after ca. 5 h, no cation **6**$^+$ could be detected at all and production of [$V(CO)_6$]$^-$ with concomitant depletion of $V(CO)_6$ became more pronounced. Combining equimolar solutions of **6**$^+$[SbF_6] and [Et_4N][$V(CO)_6$] in CH_2Cl_2 generated essentially the same FTIR pattern in ν_{CN} and ν_{CO} stretching regions.

Synthesis of [Cr(CNFc)$_6$][BF$_4$]$_2$ (5^{2+}[BF$_4$]$_2$). CH_2Cl_2 (50 mL) was introduced into a flask containing a solid mixture of **5**$^+$[BF_4] (0.500 g, 0.356 mmol) and $AgBF_4$ (0.071 g, 0.365 mmol) at room temperature. Within minutes, the initially brown reaction mixture acquired a greenish hue. After stirring for 24 h at room temperature, all but 25 mL of the solvent was removed from the forest-green solution under vacuum. Heptane (ca. 30 mL) was added with stirring to precipitate a beautiful, microcrystalline, forest-green solid. The brownish supernatant was decanted. The solid was washed with pentane (2 × 30 mL) until the washings were absolutely colorless and dried in vacuo for 1 h to afford **5**$^{2+}$[BF_4]$_2$ (0.480 g, 0.322 mmol) in a 90% yield. Compound **5**$^{2+}$[BF_4]$_2$ decomposes above 250 °C without melting. Anal. Calcd for $C_{66}H_{54}N_6B_2CrF_8Fe_6$: C, 53.14; H, 3.65; N, 5.63. Found: C, 52.47; H, 3.41; N, 5.50. IR (CH_2Cl_2): ν_{CN} 2131 vs, 2160 m sh; ν_{BF} 1065 s br cm^{-1}. ^{1}H NMR (400 MHz, CD_2Cl_2, 25 °C): δ −1.04 (s, 2H, C_5H_4, $H^{2,5}$), 3.83 (s, 5H, C_5H_5), 7.75 (s, 2H, C_5H_4, $H^{3,4}$) ppm. ^{13}C{^{1}H} NMR (100.6 MHz, CD_2Cl_2, 25 °C): δ 72.6 (C_5H_5), 97.3 (C_5H_4, $C^{3,4}$), 158.5 (C_5H_4, $C^{2,5}$) ppm. ^{14}N NMR (36.2 MHz, CD_2Cl_2, 25 °C): δ 1044.4 ($W1/2$ = 130 Hz) ppm. μ_{eff}(24.5 °C) = 2.76 μ_B (χ_{diam} = −482.4 × 10^{-6} cm^3 mol^{-1}).

Synthesis of [Cr(CNCm)$_6$][SbF$_6$]$_2$ (6^{2+}[SbF$_6$]$_2$). A colorless solution of $AgSbF_6$ (0.047 g, 0.137 mmol) in 40 mL of CH_2Cl_2 was added to a green solution of **6**$^+$[SbF_6] (0.216 g, 0.130 mmol) in 30 mL of CH_2Cl_2 with vigorous stirring at room temperature. The color of the reaction mixture changed from green to dark blue-green over a period of 1 h. The mixture was filtered through a 4 cm plug of Celite. An additional 40 mL of CH_2Cl_2 was employed to wash the filtercake until the washings were colorless. The filtrate was concentrated to about 10 mL, layered with 100 mL of heptane, and kept at −35 °C overnight. The resulting crystals were decanted and dried under vacuum for 4 h to provide moss-green **6**$^{2+}$[SbF_6]$_2$ (0.211 g, 0.111 mmol) in an 85% yield. Compound **6**$^{2+}$[SbF_6]$_2$ decomposes at 162 °C without melting. Anal. Calcd for $C_{54}H_{24}N_6CrF_{12}Mn_6O_{18}Sb_2$: C, 34.17; H, 1.27; N, 4.43. Found: C, 33.99; H, 1.15; N, 4.33. IR (CH_2Cl_2): ν_{CN} 2156 m br; ν_{CO} 2034 s, 1961 vs; ν_{SbF} 630 s cm^{-1}. ^{1}H NMR (500 MHz, CD_2Cl_2, 24 °C): δ −3.74 (s, 2H, C_5H_4, $H^{2,5}$), 6.46 (s, 2H, C_5H_4, $H^{3,4}$), ppm. ^{13}C{^{1}H} NMR (125.8 MHz, CD_2Cl_2, 24 °C): δ 91.6 (C_5H_4, $C^{3,4}$), 202.5 (*C*O), 207.3 (C_5H_4, $C^{2,5}$), ppm. ^{14}N NMR (36.2 MHz, CD_2Cl_2, 24 °C): δ 1021.3 ($W1/2$ = 878 Hz) ppm. μ_{eff}(24.0 °C) = 3.01 μ_B (χ_{diam} = −460.2 × 10^{-6} cm^3 mol^{-1}).

X-ray Crystallographic Characterization of 5·CH$_2$Cl$_2$, 6, 5$^+$[V(CO)$_6$]·CH$_2$Cl$_2$, and 5^{2+}[BF$_4$]$_2$·CH$_2$Cl$_2$. X-ray quality crystals of **5**·CH_2Cl_2 were obtained from a nearly saturated solution of **5** in CH_2Cl_2 maintained at −30 °C for two weeks. Crystals of **6**, **5**$^+$[$V(CO)_6$]·CH_2Cl_2, and **5**$^{2+}$[BF_4]$_2$·CH_2Cl_2 were grown at 4 °C by carefully layering pentane over CH_2Cl_2 solutions of these complexes. All manipulations with the crystals prior to transfer to the goniometer were performed in air. Intensity data for all samples were collected using a Bruker APEX CCD area detector mounted on a Bruker D8 goniometer employing graphite-monochromated Mo Kα radiation (λ = 0.71073 Å). The samples were cooled to 100(2) K. The space groups were determined by systematic absences

Table 1. Crystal Data, Data Collection, Solution, and Refinement for $5\cdot CH_2Cl_2$, 6, $5^+[V(CO)_6]\cdot CH_2Cl_2$, and $5^{2+}[BF_4]_2\cdot CH_2Cl_2$

	$5\cdot CH_2Cl_2$	**6**	$5^+[V(CO)_6]\cdot CH_2Cl_2$	$5^{2+}[BF_4]_2\cdot CH_2Cl_2$
empirical formula	$C_{67}H_{56}Cl_2CrFe_6N_6$	$C_{54}H_{24}CrMn_6N_6O_{18}$	$C_{73}H_{56}Cl_2CrFe_6N_6O_6V$	$C_{67}H_{56}B_2Cl_2CrF_8Fe_6N_6$
fw	1403.18	1426.43	1622.18	1576.80
cryst habbit, color	plate, red	block, red	prism, black	plate, green
cryst size (mm)	0.20 × 0.15 × 0.04	0.28 × 0.20 × 0.16	0.24 × 0.17 × 0.05	0.39 × 0.33 × 0.04
cryst syst	triclinic	triclinic	triclinic	monoclinic
space group	$P\bar{1}$	$P\bar{1}$	$P\bar{1}$	$P2_1/n$
a (Å)	9.7777(11)	12.422(3)	13.0914(7)	19.0172(12)
b (Å)	10.6494(12)	12.638(3)	16.6234(9)	21.7693(14)
c (Å)	14.6628(17)	16.810(3)	16.8244(9)	30.9281(19)
α (deg)	92.226(2)	94.215(4)	68.977(2)	90
β (deg)	95.533(2)	91.765(4)	77.423(2)	94.422(2)
γ (deg)	111.283(2)	93.017(4)	87.490(2)	90
V (Å^3)	1411.5(3)	2626.6(10)	3333.3(3)	12765.8(14)
Z, Z'	1, 0.5	2, 1	2, 1	8, 2
ρ_{calc} (Mg m^{-3})	1.651	1.804	1.616	1.641
μ (mm^{-1})	1.828	1.678	1.696	1.643
F(000)	714	1416	1642	6368
temp (K)	100(2)	100(2)	100(2)	100(2)
θ range (deg)	2.06−30.02	2.01−26.00	1.50−26.00	1.42−26.00
no. of reflns collected	10507	16688	21148	71211
no. of unique reflns	7176	9971	12396	24833
R_{int}[a]	0.0191	0.0273	0.0268	0.0372
max./min. transmn	0.9305/0.7113	0.7751/0.6508	0.9200/0.6864	0.9372/0.5666
no. of data/restraints/params	7176/43/409	9971/0/766	12 396/20/856	24 833/11/1685
no. of reflns with $I > 2\sigma(I)$	5999	8886	10032	17519
R1[b]; wR2[c]	0.0353; 0.0884	0.0365; 0.1074	0.0345; 0.0880	0.0493; 0.1330
GOF on F^2	1.023	1.047	0.942	0.974
largest diff peak/hole (e·Å^{-3})	0.768/−0.340	1.091/−0.380	1.185/−0.579	3.171/−1.457

[a] $R_{int} = \sum|F_o^2 - \langle F_o^2\rangle|/\sum|F_o^2|$. [b] $R1 = \sum||F_o| - |F_c||/\sum|F_o|$. [c] $wR2 = [\sum(w(F_o^2 - F_c^2)^2)/\sum(w(F_o^2)^2)]^{1/2}$.

and/or statistical tests and verified by subsequent refinements. All structures were solved by direct methods and refined by full-matrix least-squares methods on F^2. Non-hydrogen atoms were refined anisotropically. Hydrogen atom positions were initially determined by geometry and refined by a riding model. Hydrogen atom displacement parameters were set to 1.2 times the displacement parameters of the bonded atoms. All calculations employed the SHELXTL V5.0 suite of programs (SHELXTL-Plus V5.0, Siemens Industrial Automation, Inc, Madison, WI). In all cases, the data were corrected for absorption by a semiempirical method.[25] For $5^{2+}[BF_4]_2\cdot CH_2Cl_2$, a spurious peak of 3.17 e·Å^{-3} was located 0.878 Å from Fe(6B) in the final difference map. The above peak is likely to be a consequence of a slight disorder of this iron atom. Notably, the Fe−C distances observed for the corresponding ferrocenyl unit are very similar to those found in all other ferrocenyl moieties within $5^{2+}[BF_4]_2\cdot CH_2Cl_2$. Crystal data, data collection, solution, and refinement information for $5\cdot CH_2Cl_2$, **6**, $5^+[V(CO)_6]\cdot CH_2Cl_2$, and $5^{2+}[BF_4]_2\cdot CH_2Cl_2$ are summarized in Table 1. Full description of the crystallographic work is available in the Supporting Information. All thermal ellipsoids are drawn at the 50% probability level.

Electrochemical Measurements. Cyclic voltammetric (CV) experiments on 2×10^{-3} M solutions of **2**, **5**, **6**, and $V(CO)_6$ in CH_2Cl_2 were conducted at room temperature using an EPSILON (Bioanalytical Systems Inc., West Lafayette, IN) electrochemical workstation. The electrochemical cell was placed in an argon-filled Vacuum Atmospheres drybox. Tetrabutylammonium hexafluorophosphate (0.1 M solution in CH_2Cl_2) was used as a supporting electrolyte. Cyclic voltammograms were recorded at 22 ± 2 °C using a three-component system consisting of a platinum working electrode, a platinum wire auxiliary electrode, and a glass encased nonaqueous silver/silver chloride reference electrode. The reference Ag/Ag^+ electrode was monitored with the ferrocenium/ferrocene couple. Under the experimental conditions employed, $\Delta E_{pa,pc}$ of the FcH^+/FcH couple was 89 mV at the scan rate of 100 mV/s. This peak-to-peak separation is identical to that previously observed for the FcH^+/FcH couple at 100 mV/s in a very similar electrochemical setup, which employed a 0.2 M solution of $[^nBu_4N][PF_6]$ in CH_2Cl_2 as a supporting electrolyte.[26] IR compensation was achieved before each CV run by measuring the uncompensated solution resistance followed by incremental compensation and circuit stability testing. Background cyclic voltammograms of the electrolyte solution were recorded before adding the analytes. The half-wave potentials ($E_{1/2}$) were determined as averages of the cathodic and anodic peak potentials of reversible couples and are referenced to the FcH^+/FcH couple.[27] No significant difference (<0.01 V) between external and internal referencing with FcH^+/FcH was documented.

Computational Work. Electronic structure calculations were conducted on the compounds **3** and **4** at the all-electron density functional theory level using the Gaussian 98 program. The computations were performed using Becke's three-parameter hybrid exchange functional[28] with the LYP correlation functional.[29] The standard 6-31G split valence basis set[30] was employed in both cases, including a single d polarization function on all heavy atoms and a single p function on all hydrogen atoms.[31] The initial molecular geometries were obtained by extracting the coordinates of single CNFc and CNCm moieties from the crystal structures of $5\cdot CH_2Cl_2$ and **6**. The geometries of the C−N−C fragments were refined through quantum chemical optimization at the theory level described above. The ferrocenyl portion of CNFc was frozen during the calculations, but in a subsequent validation step, the unsubstituted ring was twisted by 36° relative to the

(25) Sheldrick, G. M. *SADABS. Program for Empirical Absorption Correction of Area Detector Data*; University of Göttingen, Germany, 2000.

(26) Zietlow, T. C.; Klendworth, D. D.; Nimry, T.; Salmon, D. J.; Walton, R. A. *Inorg. Chem.* **1981**, *20*, 947−949.

(27) Conelly, N. G.; Geiger, W. *Chem. Rev.* **1996**, *96*, 877−910.

(28) Becke, A. D. *J. Chem. Phys.* **1993**, *98*, 5648−5652.

(29) (a) Miehlich, B.; Savin, A.; Stoll, H.; Preuss, H. *Chem. Phys. Lett.* **1989**, *157*, 200−206. (b) Lee, C.; Yang W.; Parr, R. G. *Phys. Rev. B* **1988**, *37*, 785−789.

(30) Hariharan, P. C.; Pople, J. A. *Mol. Phys.* **1974**, *27*, 209−214.

(31) Frisch, M. J.; Pople, J. A.; Binkley, J. S. *J. Chem. Phys.* **1984**, *80*, 3265−3269.

Scheme 1

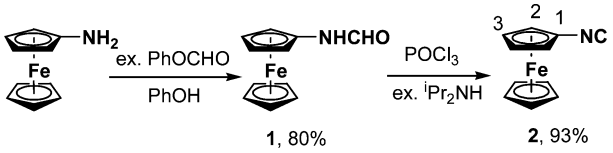

substituted ring in order to confirm that ring rotations play a negligible role in the structure and energetics of the Frontier orbitals. All computational parameters not explicitly specified above were set to their default values.

Results and Discussion

Synthetic Work. Several greatly improved syntheses of aminoferrocene, which afford multigram quantities of H_2NFc in up to 52% yields starting from ferrocene, have recently been published.[14] Our facile preparation of thermally stable, peach-colored isocyanoferrocene (**2**) involved treatment of solid $FcNH_2$ with a 65/35 mol % mixture of phenyl formate/phenol, followed by dehydration of the resulting ferrocenylformamide (**1**) with *strictly* 1.0 equiv of $POCl_3$ in the presence of $^iPr_2NH$ in CH_2Cl_2 (Scheme 1). The superior formylating potency of phenyl formate as compared to EtOC(O)H permitted us to conduct the formylation step at ambient temperature, thereby preventing previously encountered[9a] extensive thermal decomposition of **1**. A solution of excess acetic-formic anhydride in CH_2Cl_2 proved equally efficient in formylating aminoferrocene at ca. 20 °C. While syntheses of isocyanides from the corresponding formamides often employ excess dehydrating agents,[1] it is imperative to avoid exposing **1** to even a slight excess of $POCl_3$ to ensure the essentially quantitative conversion of **1** into **2**. This observation might explain the earlier report by others claiming that dehydration of FcNHCHO with $POCl_3$ afforded "variable, nonreproducible (25−90%) yields" of CNFc.[9a]

To demonstrate the feasibility of varying the transition metal moiety bound to the isocyanocyclopentadienyl ring, synthesis of isocyanocymantrene (**4**) was sought. The choice of the "$Mn(CO)_3$" unit was in part influenced by the fact that, among the cyclopentadienyl complexes of metals, cymantrene derivatives are second only to those of ferrocene in terms of synthetic applications.[32] Aminocymantrene, the most obvious precursor to **4**, can be prepared via a laborious, six-step reaction sequence, $CmH \rightarrow CmC(O)C_6H_4$-*p*-$Cl \rightarrow CmC(O)OH \rightarrow CmC(O)Cl \rightarrow CmC(O)N_3 \rightarrow CmNHC(O)OCH_2Ph \rightarrow CmNH_2$, in 11%−26% yields.[24,33]

In search for a more practical route to $CmNH_2$, we treated in situ-generated lithiocymantrene with tosyl azide to afford somewhat thermally sensitive CmN_3 (Scheme 2). Without isolation, cymantrenyl azide was reduced to $CmNH_2$ in a good yield using $NaBH_4$.[34] The crude amine was then formylated with acetic-formic anhydride to give pure CmNHC(O)H (**3**) in a 55% overall yield (starting from cymantrene) after workup. In dichloromethane solution at 25 °C, **3** exists as a 9:1 mixture of two conformational isomers, presumably due to the restricted rotation[35] around the Cm(H)N−C(O)H bond. Dehydration of **3** under standard conditions (Scheme 2) provided thermally and light sensitive, tan-yellow **4**. For long-term storage, compound **4** should be cooled to ca. −30 °C to avoid substantial thermal decomposition of its samples.

Scheme 2

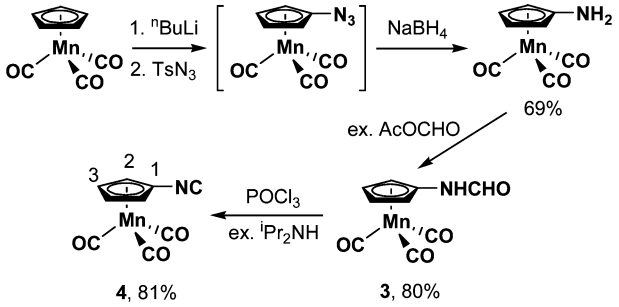

Scheme 3

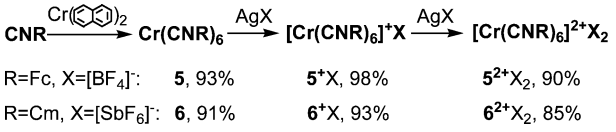

Table 2. Characteristic IR,[a] ^{13}C NMR,[b] and ^{14}N NMR[c] Data for 2 and 4 at 25 °C

	ν_{CN}, cm^{-1}	$\delta\{^{13}CNR\}$, ppm	$\delta\{C^{14}NR\}$, ppm
2	2122	174.0	172.1
4	2133	168.9	164.3

[a] In CH_2Cl_2. [b] In $CDCl_3$ vs Me_4Si. [c] In $CDCl_3$ vs liquid NH_3.

The entire synthesis of **4** from cymantrene can be conveniently monitored by IR in the ν_{CO}, ν_{NN}, ν_{NH}, and ν_{CN} stretching regions. Unlike CNPh,[6,7] both **2** and **4** are air stable for practical purposes and do not show a tendency to rearrange into the corresponding nitriles. Isocyanides **2** and **4** can be easily distinguished from FcCN and CmCN, respectively, on the basis of the characteristic features in their IR (ν_{CN}), ^{13}C NMR ($\delta\{CNR\}$), and ^{14}N NMR ($\delta\{CNR\}$) spectra (Table 2).

Combining 6 equiv of **2** with $Cr(\eta^6\text{-naphthalene})_2$[22] in THF afforded crystalline, orange-red $Cr(CNFc)_6$ after workup (**5**) (Scheme 3). Oxidation of **5** with 1.0 equiv of $AgBF_4$ in CH_2Cl_2 gave saddle-brown microcrystals of $[Cr(CNFc)_6][BF_4]$ ($\mathbf{5}^+[BF_4]$), subsequent treatment of which with another equivalent of $AgBF_4$ in CH_2Cl_2 provided $[Cr(CNFc)_6][BF_4]_2$ ($\mathbf{5}^{2+}[BF_4]_2$) as a sparkling, forest-green solid (Scheme 3). High yields of microcrystalline, scarlet $Cr(CNCm)_6$ (**6**), lime-green $[Cr(CNCm)_6][SbF_6]$ ($\mathbf{6}^+[SbF_6]$), and moss-green $[Cr(CNCm)_6][SbF_6]_2$ ($\mathbf{6}^{2+}[SbF_6]_2$) were obtained from **4** in a similar fashion (Scheme 3).

Infrared and magnetic properties of $Cr(CNR)_6$, $[Cr(CNR)_6]^+$, and $[Cr(CNR)_6]^{2+}$ (R = Fc, Cm) are fully consistent with their formulations as low-spin, octahedral complexes of Cr(0), Cr(I), and Cr(II), respectively (Table 3). The energy of the "T_{1u}"-like ν_{CN} band increases upon going from **5** to $\mathbf{5}^+$ to $\mathbf{5}^{2+}$. This indicates sequential oxidation of the chromium rather than the iron atoms.

(32) Ginzburg, A. G. Chemistry of Cymantrene. *Russ. Chem. Rev.* **1993**, *62*, 1098−1118.

(33) Our attempts to scale-up the reported procedures by a factor of 5 resulted in the overall yield reduction from 26 to 11%.

(34) Notably, recent attempts by others to reduce cymantrenyl azide with $NaBH_4$ have failed to generate any $CmNH_2$: Sünkel, K.; Birk, U.; Soheili, S.; Stramm, C.; Teuber, R. *J. Organomet. Chem.* **2000**, *599*, 247−255.

(35) Kessler, H. *Angew. Chem., Int. Ed. Engl.* **1970**, *9*, 219−235.

Table 3. IR[a] and Magnetic Data[b] for 5^z and 6^z (z = 0, 1+, 2+)

	ν_{CN}, cm^{-1}	ν_{CO}, cm^{-1}	μ_{eff}(25 °C), μ_B
5	1971		diamagnetic
6	1947	2030, 1937	diamagnetic
$\mathbf{5}^{+}$ [c]	2053		1.78
$\mathbf{6}^{+}$ [d]	2073	2029, 1950	1.99
$\mathbf{5}^{2+}$ [c]	2131		2.76
$\mathbf{6}^{2+}$ [d]	2156	2034, 1961	3.01

[a] In CH_2Cl_2. [b] Solid state. [c] $[BF_4]^-$ salt. [d] $[SbF_6]^-$ salt.

The same trend in ν_{CN} was documented for **6**, $\mathbf{6}^{+}$, and $\mathbf{6}^{2+}$. The C−NR stretching frequencies of **5**, $\mathbf{5}^{+}$, **6**, and $\mathbf{6}^{+}$ are significantly depressed with respect to those of the corresponding free isocyanides, reflecting substantial back-bonding interactions within these complexes.[36] In addition, the energy of the asymmetric ν_{CO} band increases by 11−13 cm^{-1} upon each one-electron oxidation of **6** to successively generate $\mathbf{6}^{+}$ and $\mathbf{6}^{2+}$. Thus, the carbonyl stretching frequencies are quite sensitive to the chromium oxidation state in $[Cr(CNCm)_6]^z$ (z = 0, 1+, 2+). Compounds $\mathbf{5}^{+}[BF_4]$, $\mathbf{6}^{+}[SbF_6]$, $\mathbf{5}^{2+}[BF_4]_2$, and $\mathbf{6}^{2+}[SbF_6]_2$ are paramagnetic both in the solid state and in solution, and their magnetic moments are in accord with low-spin d^5 configuration of $\mathbf{5}^{+}$ and $\mathbf{6}^{+}$ and low-spin d^4 configuration of $\mathbf{5}^{2+}$ and $\mathbf{6}^{2+}$.

The remarkable air, light, and thermal stabilities of **5**, **6**, $\mathbf{5}^{+}$, $\mathbf{6}^{+}$, $\mathbf{5}^{2+}$, and $\mathbf{6}^{2+}$ constitute compelling evidence that the nonbenzenoid, η^5-cyclopentadienyl substituents in **2** and **4** are much closer to a benzenoid aryl rather than an alkyl group in terms of their electronic influence. Indeed, species $[Cr(CNAr)_6]^{0,1+,2+}$ are generally air and thermally stable in the solid state.[36] On the contrary, the only two binary alkyl isocyanides of Cr(0) known, namely, $Cr(CN^tBu)_6$ and $Cr(CNC_6H_{11})_6$, are very air and light sensitive.[22b,37] Furthermore, species $[Cr(CNAlkyl)_6]^+$ have been observed only electrochemically and are too thermally unstable to be isolated.[38] Similar to $[Cr(CNAr)_6]^{2+}$, $\mathbf{5}^{2+}$ and $\mathbf{6}^{2+}$ are reluctant to add another isocyanide ligand, whereas seven-coordinate $[Cr(CNAlkyl)_7]^{2+}$ (alkyl = ^{t}Bu, C_6H_{11}) are well documented.[38]

Complex **5** was readily oxidized by vanadium(0) hexacarbonyl in CH_2Cl_2 to afford $\mathbf{5}^{+}[V(CO)_6]$ in a nearly quantitative yield (eq 1). The electron transfer was complete within minutes as judged by FTIR of the reaction mixture. The spectroscopic characteristics of the cations within $\mathbf{5}^{+}[V(CO)_6]$ and $\mathbf{5}^{+}[BF_4]$ are identical. On the other hand, the FTIR spectrum of the mixture obtained by combining equimolar solutions of **6** and $V(CO)_6$ in CH_2Cl_2 (eq 2) was dominated by bands due to the neutral starting materials and indicated the presence of only trace amounts of ions $\mathbf{6}^{+}$ and $[V(CO)_6]^-$. The same FTIR pattern in ν_{CO} and ν_{CN} regions was generated by treating $\mathbf{6}^{+}[SbF_6]$ with 1 equiv of $[Et_4N][V(CO)_6]$ (eq 3). Thus, the redox equilibrium shown in eq 2 is greatly shifted to the left. Over time, the already minute presence of cation $\mathbf{6}^{+}$ in the mixtures described by eqs 2 and 3 could not be detected at all, while the ν_{CO} band at 1853 cm^{-1} due to $[V(CO)_6]^-$ appeared more prominent compared to that observed shortly after mixing the reagents. Both of these observations are consistent with slow thermal decomposition of $V(CO)_6$ in dichloromethane at ambient temperature to generate $[V(CO)_6]^-$.[19]

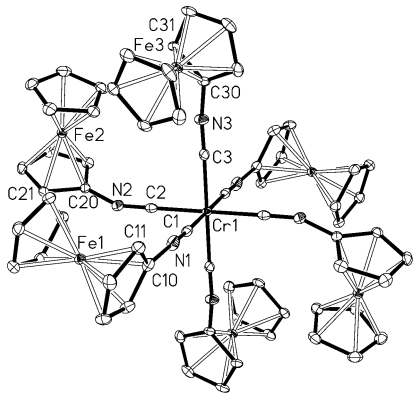

Figure 1. ORTEP (50%) diagram of $\mathbf{5}\cdot CH_2Cl_2$. Hydrogen atoms and solvent are omitted for clarity. Selected bond distances (Å) and angles (deg): Cr−C1 1.930(2), Cr−C2 1.941(2), Cr−C3 1.941(2), C1−N1 1.175(3), C2−N2 1.183(3), C3−N3 1.177(3), av C−N−C 161.5.

$$\mathbf{5} + V(CO)_6 \xrightarrow[94\%]{} \mathbf{5}^{+}[V(CO)_6] \quad (1)$$

$$\mathbf{6} + V(CO)_6 \rightleftharpoons \mathbf{6}^{+}[V(CO)_6] \quad (2)$$

$$\mathbf{6}^{+}[SbF_6] + [Et_4N][V(CO)_6] \rightleftharpoons \mathbf{6} + V(CO)_6 + [Et_4N][SbF_6] \quad (3)$$

Crystallographic Studies. Complexes $\mathbf{5}^z$ and $\mathbf{6}^z$ (z = 0, 1+, 2+) are highly unusual owing to the incorporation of seven transition metals within relatively compact ML_6 motifs. In addition, compounds **5**, $\mathbf{5}^{+}$, and $\mathbf{5}^{2+}$ feature seven electroactive metal centers (vide infra). To the best of our knowledge, only one other species containing six ferrocenyl groups separated from the central metal ion by no more than two atoms is known.[39] The X-ray structure of $\mathbf{5}\cdot CH_2Cl_2$ is shown in Figure 1.[10] The metric parameters of its nearly perfectly octahedral $Cr(CN)_6$ core are in accord with those observed for other binary isocyanides of chromium(0).[37,40] The average C−N−C(Fc) angle in **5** is 162°. Such a degree of bending at the nitrogen atom is also typical for zerovalent, octahedral complexes of bulky aryl isocyanides (aryl = 2,6-$Me_2C_6H_4$, 2,6-$^iPr_2C_6H_4$).[40a,41] Notably, the average C−N−C(^{t}Bu) angle in $Cr(CN^tBu)_6$ is 153°.[37] The less pronounced bending of aryl-substituted isocyanide ligands in their low-valent complexes has been attributed to partial delocalization of the back-donated electron density into the aromatic rings that can be described by the linear resonance structures M=C=N^+=$Aryl^-$.[2a,b]

(36) (a) Bullock, J. P.; Mann, K. R. *Inorg. Chem.* **1989**, *28*, 4006−4011. (b) Treichel, P. M.; Essenmacher, G. J. *Inorg. Chem.* **1976**, *15*, 146−150.

(37) Acho, J. A.; Lippard, S. J. *Organometallics* **1994**, *13*, 1294−1299.

(38) (a) Mialki, W. S.; Wigley, D. E.; Wood, T. E.; Walton, R. A. *Inorg. Chem.* **1982**, *21*, 480−485. (b) Dewan, J. C.; Mialki, W. S.; Walton, R. A.; Lippard, S. J. *J. Am. Chem. Soc.* **1982**, *104*, 133−136.

(39) This is a Cd(II) complex of 1,4,7,10,13,16-hexa(ferrocenylmethyl)-1,4,7,10,13,16-hexaaza-cyclooctadecane: Lloris, J. M.; Martinez-Mañez, R.; Pardo, T.; Soto, J.; Padilla-Tosta, M. E. *J. Chem. Soc., Dalton Trans.* **1998**, 2635−2641.

(40) (a) Anderson, K. A.; Scott, B.; Wherland, S.; Willett, R. D. *Acta Crystallogr.* **1991**, *C47*, 2337−2339. (b) Ljungström, E. *Acta Chem. Scand.* **1978**, *A32*, 47−50.

(41) Barybin, M. V.; Young, V. G., Jr.; Ellis, J. E. *J. Am. Chem. Soc.* **2000**, *122*, 4678−4691, and references therein.

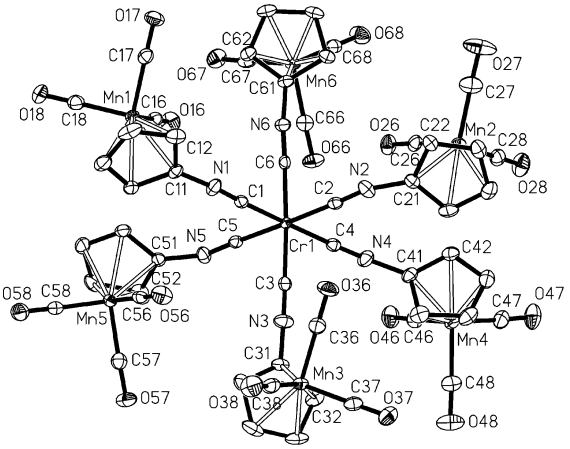

Figure 2. ORTEP (50%) diagram of **6**. Hydrogen atoms and solvent are omitted for clarity. Selected bond distances (Å) and angles (deg): Cr−C1 1.951(2), Cr−C2 1.910(2), Cr−C3 1.930(2), Cr−C4 1.907(2), Cr−C5 1.926(2), Cr−C6 1.937(2), C1−N1 1.167(3), C2−N2 1.179(3), C3−N3 1.168(3), C4−N4 1.193(3), C5−N5 1.178(3), C6−N6 1.175(3), C1−N1−C10 169.6(2), C2−N2−C20 155.6(2), C3−N3−C30 176.3(3), C4−N4−C40 139.5(2), C5−N5−C50 157.3(2), C6−N6−C60 173.7(2).

Table 4. Selected Average Metric Parameters for 6, 5, 5^+, and 5^{2+}[a]

	Cr−C, Å	C−NR, Å	C−N−C, deg
6	1.93(2)	1.18(1)	162(14)
5	1.937(7)	1.178(5)	162(4)
$\mathbf{5}^+$	1.972(13)	1.160(3)	171(4)
$\mathbf{5}^{2+}$ [b]	2.019(17)	1.150(5)	175(3)

[a] Numbers in parentheses constitute the standard deviations of the mean. [b] Both crystallographically independent cations within $\mathbf{5}^{2+}[BF_4]_2{\cdot}CH_2Cl_2$ are considered.

The shortest Fe···Fe distance within **2** is 6.29 Å, which is only 0.93 Å greater than that in zwitterionic Fc_4B.[42]

Figure 2 displays the molecular structure of **6**. While the average Cr−C and C−NCm bond distances and C−N−C angle for **6** are virtually identical to the corresponding values found for **5**, complex **6** exhibits greater variations among the *individual* parameters of the same chemical nature (Figure 2, Table 4). The lack of crystallographically imposed symmetry in **6** coupled with the somewhat greater bulk of CNCm compared to CNFc may account for the above observation. A very similar phenomenon was noted for the structure of $Cr(CN^tBu)_6$, in which all bulky CN^tBu ligands are crystallographically unique.[37] Indeed, in $Cr(CN^tBu)_6$, the Cr−C distances vary from 1.87(1) to 1.98(1) Å and the C−N−C angles range from severely bent, 136.1(9)°, to nearly linear, 175(1)°.[37] In both **6** and $Cr(CN^tBu)_6$, smaller C−N−C angles correspond to shorter Cr−C bonds. The shortest Cr···Mn and Mn···Mn distances within **6** are 5.61 and 6.14 Å, respectively.

Crystallographic characterization of $\mathbf{5}^+[V(CO)_6]$ (Figure 3) confirmed the electron transfer from **5** to $V(CO)_6$ upon mixing the two electroneutral compounds (eq 1). The data for $\mathbf{5}^+$ are very similar to those recently determined by us for $[Cr(CN^2Az)_6]^+$ (^{2}Az = 2-azulenyl). Table 4 shows that the Cr−C bonds lengthen, the C−NFc distances shorten, and the C−N−C(Fc) angles

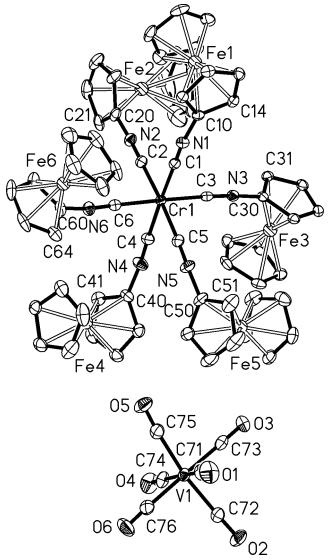

Figure 3. ORTEP (50%) diagram of $\mathbf{5}^+[V(CO)_6]{\cdot}CH_2Cl_2$. Hydrogen atoms and solvent are omitted for clarity. Selected bond distances (Å) and angles (deg): Cr−C1 1.971(3), Cr−C2 1.994(3), Cr−C3 1.979(3), Cr−C4 1.957(3), Cr−C5 1.963(3), Cr−C6 1.971(3), V−C71 1.935(3), V−C72 1.959(3), V−C73 1.961(3), V−C74 1.974(3), V−C75 1.953(3), V−C76 1.953(3), C1−N1 1.158(3), C2−N2 1.157(3), C3−N3 1.164(3), C4−N4 1.160(3), C5−N5 1.159(3), C6−N6 1.163(3), C71−O1 1.148(4), C72−O2 1.150(3), C73−O3 1.151(4), C74−O4 1.147(4), C75−O5 1.160(4), C76−O6 1.149(4), C1−N1−C10 167.4(3), C2−N2−C20 176.9(3), C3−N3−C30 176.2(3), C4−N4−C40 167.0(3), C5−N5−C50 169.7(3), C6−N6−C60 169.9(3).

increase upon oxidation of **5** to $\mathbf{5}^+$. These facts imply a lower extent of back-bonding within less electron-rich $\mathbf{5}^+$ as compared to **5**. The Cr−C, C−NR, and C−N−C(R) values obtained for $\mathbf{5}^+$ are very similar to those recently determined by us for $[Cr(CN^6Az)_6]^+$ (^{6}Az = 6-azulenyl), another binary Cr(I) complex of a nonbenzenoid aromatic isocyanide.[13] The V−C bond lengths within the nearly octahedral anion of $\mathbf{5}^+[V(CO)_6]$ vary from 1.935(3) to 1.974(3) Å and are statistically shorter than those reported for neutral $V(CO)_6$ (1.993(2)−2.005(2) Å).[43] On the other hand, they are either indistinguishable from or only marginally longer than the V−C distances found for several other structurally characterized salts of $[V(CO)_6]^-$.[44] The C−O bond lengths in $\mathbf{5}^+[V(CO)_6]$ (1.147(4)−1.160(4) Å) are well within the range of the C−O distances previously documented for $[V(CO)_6]^-$.[44] Compound $\mathbf{5}^+[V(CO)_6]$ belongs to a fundamentally intriguing class of ion pairs $A^+|[V(CO)_6]^-$, some of which have been shown to undergo interionic electron transfer upon photoexcitation.[45]

One of two crystallographically unrelated, 16-electron dications $\mathbf{5}^{2+}$ within $\mathbf{5}^{2+}[BF_4]_2{\cdot}CH_2Cl_2$ is shown in Figure 4. As summarized in Table 4, the Cr−C bonds continue to elongate, while the C−NFc bonds be-

(42) Cowan, D. O.; Shu, P.; Hedberg, F. L.; Rossi, M.; Kistenmacher, T. J. *J. Am. Chem. Soc.* **1979**, *101*, 1304−1307.

(43) Bellard, S.; Rubinson, K. A.; Sheldrick, G. M. *Acta Crystallogr.* **1979**, *B47*, 271−274.

(44) (a) Doyle, G.; Eriksen, K. A.; Van Engen, D. *Organometallics* **1985**, *4*, 2201−2206. (b) Calderazzo, F.; Pampaloni, G.; Lanfranchi, M.; Pelizzi, G. *J. Organomet. Chem.* **1985**, *296*, 1−13. (c) Calderazzo, F.; Pampaloni, G.; Vitali, D.; Zanazzi, P. F. *J. Chem. Soc., Dalton Trans.* **1982**, 1993−1997. (d) Silverman, L. D.; Corfield, P. W. R.; Lippard, S. J. *Inorg. Chem.* **1981**, *20*, 3106−3109. (e) Wilson, R. D.; Bau, R. *J. Am. Chem. Soc.* **1974**, *96*, 7601−7602.

(45) Marlin, T. W.; Homoelle, B. J.; Spears, K. G. *J. Phys. Chem. A* **2002**, *106*, 1152−1166.

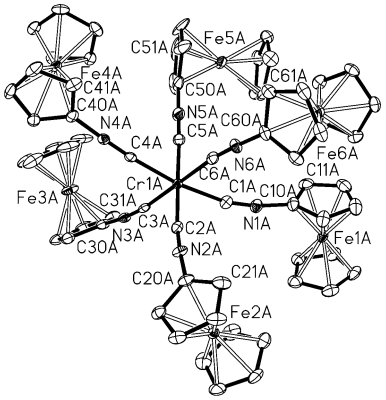

Figure 4. ORTEP (50%) diagram of $\mathbf{5}^{2+}[BF_4]_2 \cdot CH_2Cl_2$. The $[BF_4]^-$ anions, solvent, and hydrogen atoms are omitted for clarity. One of two independent cations is shown. Selected bond distances (Å) and angles (deg): CrA−C1A 2.043(4), CrA−C2A 2.010(4), CrA−C3A 1.974(7), CrA−C4A 2.035(4), CrA−C5A 2.013(4), CrA−C6A 2.004(4), C1A−N1A 1.158(5), C2A−N2A 1.149(5), C3A−N3A 1.155(4), C4A−N4A 1.154(4), C5A−N5A 1.151(5), C6A−N6A 1.151(5), C1A−N1A−C10A 169.8(4), C2A−N2A−C20A 175.5(4), C3A−N3A−C30A 171.7(4), C4A−N4A−C40A 175.2(4), C5A−N5A−C50A 178.2(5), C6A−N6A−C60A 176.5(4).

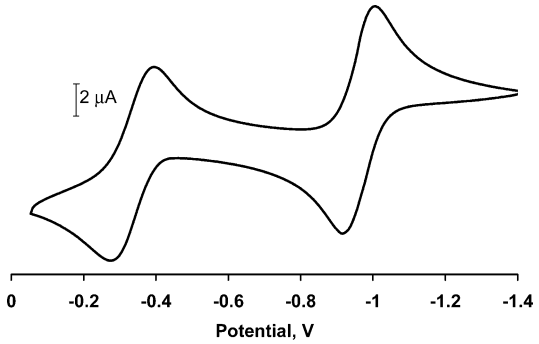

Figure 5. Cyclic voltammogram of **5** in 0.1 M $[^nBu_4N][PF_6]$/CH_2Cl_2 at negative potentials vs FcH/FcH^+. Scan rate = 100 mV/s.

come shorter in the oxidation process $\mathbf{5} \rightarrow \mathbf{5}^+ \rightarrow \mathbf{5}^{2+}$. Thus, the first two oxidations of **5** are chromium-centered. The trends in the bond distances and angles presented in Table 4 nicely parallel those documented for $[Cr(CNPh)_6]^z$ (z = 0, 1+, 2+)[40b,46] and the isoelectronic series $[V(CN\text{-}2,6\text{-}Me_2C_6H_3)_6]^z$ (z = 1−, 0, 1+).[41]

Electrochemical and DFT Studies. Cyclic voltammograms of **5** and **6** in CH_2Cl_2/$[^nBu_4N][PF_6]$ solutions exhibit two one-electron, successive, quasi-reversible[47] anodic waves ($\Delta E_{pc,pa}$ = 79−88 mV at ν = 100 mV/s, $i_c/i_a \approx 1.0$; Figures 5 and 6). These waves correspond to the chromium-centered oxidations consecutively generating the cations $[Cr^I(CNR)_6]^+$ and $[Cr^{II}(CNR)_6]^{2+}$ (R = Fc, Cm). The electrochemical data summarized in Table 5 imply that the donor/acceptor ratio[2b] of the isocyanide ligands decreases substantially in the order $CNC_6H_{11} \ll CNFc < CNPh \ll CNCm$.

The influence of π-back-bonding on $E_{1/2}$ values of the Cr^z/Cr^{z+1} couples should be greatest in the case of the electron-rich Cr^0/Cr^I systems, whereas the relative contribution of σ(RNC→Cr) donation to the donor/acceptor ratio of CNR should increase upon oxidation. Taking into account both data rows of Table 5, one may suggest that CNCm is a significantly stronger π-acceptor and, perhaps, a slightly weaker σ-donor than CNFc. To further corroborate this conclusion, we considered DFT-generated molecular orbitals of **2** and **4**. From Figure 7 it is apparent that virtual MOs of **4** capable of back-bonding (LUMO, LUMO+3, and LUMO+6; LUMO = lowest unoccupied molecular orbital) show substantially greater stabilization compared to the corresponding virtual MOs of **2** (LUMO, LUMO+2, LUMO+3), thereby making CNCm a stronger π-acid than CNFc. In addition, the HOMO-7 (HOMO = highest occupied molecular orbital) of **4**, localized primarily on the terminal carbon atom (lone pair) and antibonding with respect to the C−NR bond, is ca. 0.5 eV more stabilized than the similar molecular orbital (HOMO-7) of **2** as illustrated in Figure 7. Therefore, CNCm would indeed be a somewhat weaker σ-donor than CNFc.

The difference in reactivity of **5** and **6** toward $V(CO)_6$ is easily rationalized by comparing $E_{1/2}$ of the couples $\mathbf{5}/\mathbf{5}^+$ and $\mathbf{6}/\mathbf{6}^+$ (Table 5) to that of $V(CO)_6/[V(CO)_6]^-$ under identical electrochemical conditions. We observed a half-wave potential of −0.54 V ($\Delta E_{pa,pc}$ = 117 mV) for the $V(CO)_6/[V(CO)_6]^-$ process in CH_2Cl_2/$[^nBu_4N][PF_6]$,[50] which is certainly high enough to ensure essentially complete[27] oxidation of **5** to $\mathbf{5}^+$ according to eq 1. On the contrary, only partial oxidation of **6** by $V(CO)_6$ might be expected at best. Of note, applying the Nernst equation to the *quasi-reversible* systems $\mathbf{6}/\mathbf{6}^+$ and $V(CO)_6/[V(CO)_6]^-$ and approximating their $E^{o\prime}$ potentials with the corresponding $E_{1/2}$ values[27] leads to an underestimation of the completeness of the actual *chemical* redox process described by eq 2.

The above electrochemical analysis indicates that the donor/acceptor characteristics of isocyanoferrocene are

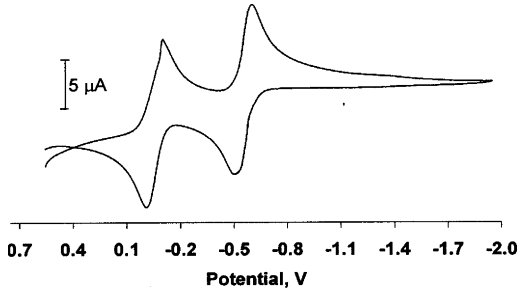

Figure 6. Cyclic voltammogram of **6** in 0.1 M $[^nBu_4N][PF_6]$/CH_2Cl_2 vs FcH/FcH^+. Scan rate = 100 mV/s.

Table 5. $E_{1/2}$ Potentials[a] (in V) for $[Cr(CNR)_6]^{z/z+1}$ versus $[FcH]^0/[FcH]^+$

	R			
couple	C_6H_{11}[b]	Fc	Ph[c]	Cm
$[Cr(CNR)_6]^{0/1+}$	−1.54	−0.97	−0.83	−0.53
$[Cr(CNR)_6]^{1+/2+}$	−0.77	−0.35	−0.21	−0.04

[a] All measurements were performed in CH_2Cl_2/$[^nBu_4N][PF_6]$ to ensure quantitative comparison. [b] Ref 48. [c] Ref 49a.

(46) Bohling, D. A.; Mann, K. R. *Inorg. Chem.* **1984**, *23*, 1426−1432.
(47) Qualitatively, these waves can be considered reversible given that, under the experimental conditions employed, reversible couple FcH/FcH^+ exhibits $\Delta E_{pc,pa}$ = 89 mV at ν = 100 mV, and this peak-to-peak separation increases upon increase in the scan rate. See also ref 26.
(48) Mialki, W. S.; Wigley, D. E.; Wood, T. E.; Walton, R. A. *Inorg. Chem.* **1982**, *21*, 480−485.
(49) (a) Bullock, J. P.; Mann, K. R. *Inorg. Chem.* **1989**, *28*, 4006−4011. (b) Treichel, P. M.; Essenmacher, G. J. *Inorg. Chem.* **1976**, *15*, 146−150.
(50) See Supporting Information.

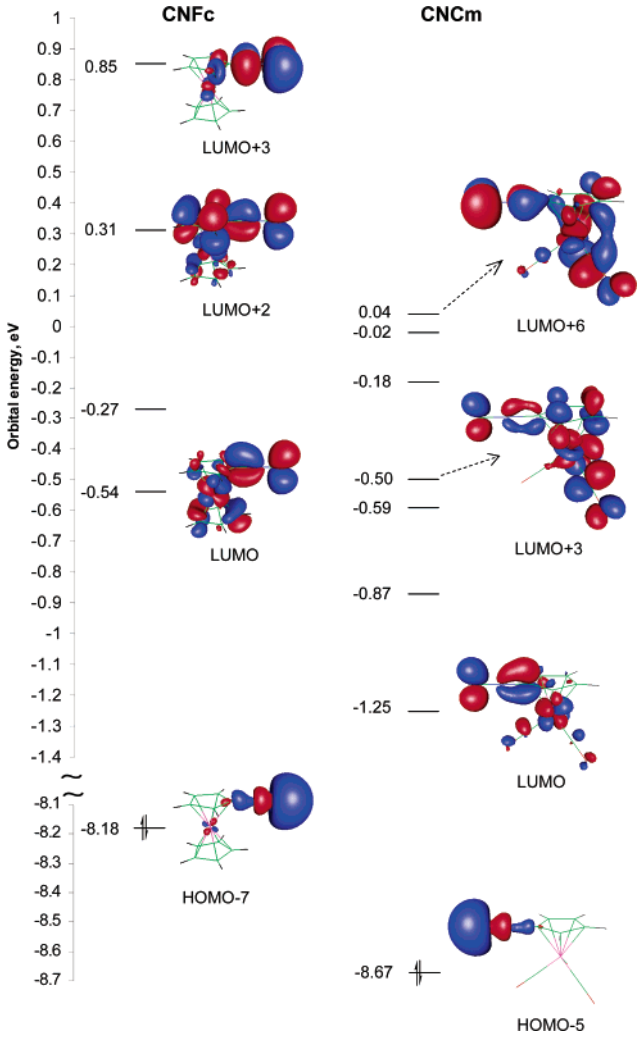

Figure 7. Selected molecular orbitals of **2** (left) and **4** (right) and their corresponding energies calculated at the 6-31G (D, F) level. For clarity, structures of orbitals with no appreciable density on the isocyano group are not shown.

much closer to those of aryl rather than alkyl isocyanides. In accord with this finding, the $E_{1/2}$ potential of the *elusive* $[Cr(CNMe)_6]^{0/1+}$ couple in CH_2Cl_2 was predicted to be −1.67 eV vs FcH/FcH^+,[51] which is 0.7 eV more negative than that of the $[Cr(CNFc)_6]^{0/1+}$ system. Thus, isocyanoferrocene is a substantially stronger π-acceptor compared to isocyanomethane, so the previously suggested[9b,c] electronic similarity between CNFc and CNMe only applies to the donor properties of these isocyanides. The enhanced π-acidity of **2** with respect to CNMe is associated with the possibility of partial delocalization of back-donated electron density into the ferrocenyl moieties of CNFc. Figure 7 illustrates that CNFc's LUMO and LUMO+2 are especially suited for such an interaction.

Application of higher potentials to a solution of **5** produced a broad anodic peak at $E_{p,a} = 0.42$ eV (Figure 8) with a shape indicative of a diffusion-controlled process. This wave corresponds to the oxidation of six ferrocenyl substituents in $\mathbf{5}^{2+}$.[52] Interestingly, a larger response was observed on the reverse cathodic scan. The symmetrical shape of the reduction wave suggests a

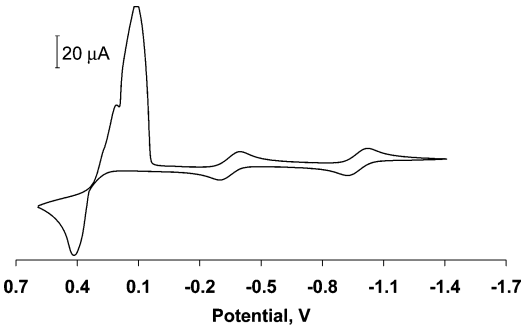

Figure 8. Cyclic voltammogram of **5** in 0.1 M $[^nBu_4N][PF_6]$/CH_2Cl_2 vs FcH/FcH^+ showing all accessible oxidation steps. Scan rate = 100 mV/s.

non-diffusion-controlled process involving the oxidation product adsorbed or precipitated onto the electrode surface.[53] Such an adsorption was very likely to be a consequence of poor solubility of the highly charged cation $[Cr(CNFc)_6]^{8+}$ in CH_2Cl_2. Upon reduction of the surface-confined octa-cation $[Cr(CNFc)_6]^{8+}$ on the reverse scan, the resultant $\mathbf{5}^{2+}$ dissolved and was further reduced under diffusion control to sequentially generate $\mathbf{5}^+$ and **5**. Importantly, practically no loss of current was documented for the Cr-centered reductions as compared to the corresponding oxidation processes on the forward scan. The cyclic voltammogram displayed in Figure 8 remained essentially unchanged upon completion of several full cycles. The average $E_{1/2}$ potential of the Fe(II)/Fe(III) transformations for $[Cr(CNFc)_6]^{z/z+1}$ is estimated to be 0.26 eV. Without commenting on the thermodynamic significance of this value, we note that it is very similar to $E_{1/2} = 0.25$ eV ($\Delta E_{pa,pc} = 150$ mV at $\nu = 100$ mV/s) observed in the electrochemical oxidation of free CNFc under the same conditions.

Multinuclear Paramagnetic NMR Studies. The paramagnetic complexes $\mathbf{5}^+$, $\mathbf{6}^+$, $\mathbf{5}^{2+}$, and $\mathbf{6}^{2+}$ give relatively narrow ^1H, ^{13}C, and ^{14}N NMR signals. This fact is consistent with their ideal ^2T ($\mathbf{5}^+$ and $\mathbf{6}^+$) and ^3T ($\mathbf{5}^{2+}$ and $\mathbf{6}^{2+}$) ground states characterized by short electron spin relaxation times, T_{1e}.[54,55] The ^1H paramagnetic shifts for $\mathbf{5}^z$ and $\mathbf{6}^z$ ($z = 1+, 2+$), determined relative to the chemical shifts of the corresponding nuclei in the diamagnetic zerovalent **5** or **6**, exhibit approximately Curie behavior at 200 K < T < 300 K (i.e., $\Delta\delta \propto 1/T$ and $\Delta\delta\{T=\infty\} \approx 0$) and are practically contact in origin because of the high symmetry of the complexes (e.g., Figure 9). Small Jahn−Teller distortions expected for these cations are very likely to be dynamic on the NMR time scale.[54]

The ^1H paramagnetic shifts for the C_5H_4 rings of $\mathbf{5}^z$ and $\mathbf{6}^z$ ($z = 1+, 2+$) are large and occur in both directions (Table 6). This suggests unpaired spin delocalization within their π-systems.[54] Given that the nature of the substituent R′ in diamagnetic (η^5-C_5H_4R')-

(51) Bursten, B. E. *J. Am. Chem. Soc.* **1982**, *104*, 1299−1304.

(52) For the $[Cr(CNFc)_6]^z$ system, the Cr(II)/Cr(III) oxidation (if it is possible at all) is expected to occur at a much more positive potential as compared to the Fe(II)/Fe(III) processes. See ref 49.

(53) Bond, A. M.; Colton, R.; Mahon, P. J.; Snook, G. A.; Tan, W. T. *J. Phys. Chem. B* **1998**, *102*, 1229−1234.

(54) LaMar, G. N., Horrocks, W. D., Jr., Holm, R. H., Eds. *NMR of Paramagnetic Molecules*; Academic Press: New York, 1973.

(55) For a discussion of theory of the paramagnetic shift for strong field d^5 complexes, see: McGarvey, B. R.; Batista, N. C.; Bezerra, C. W. B.; Schultz, M. S.; Franco, D. W. *Inorg. Chem.* **1998**, *37*, 2865−2872, and references therein.

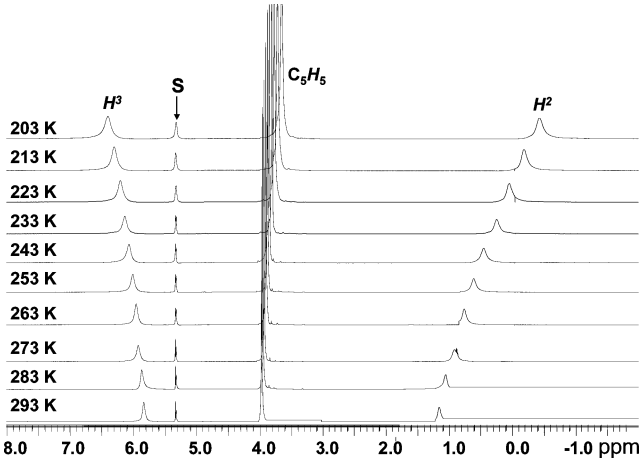

Figure 9. Variable-temperature ^{1}H NMR spectra of $\mathbf{5}^+[BF_4]$ in CD_2Cl_2 at 500 MHz.

Table 6. ^{1}H, ^{13}C, and ^{14}N NMR Paramagnetic Shifts[a] (in ppm) for $\mathbf{5}^+$, $\mathbf{6}^+$, $\mathbf{5}^{2+}$, and $\mathbf{6}^{2+}$

	$H^{2,5}$	$H^{3,4}$	C_5H_5	$C^{2,5}$	$C3,4$	C_5H_5	CO	N
$\mathbf{5}^{+\,b}$	−2.95	+1.55	−0.36	+41.6	+9.9	+0.9		+553.1
$\mathbf{6}^{+\,c}$	−4.7	+1.32		+66.3	+6.3		−7.5	+697.1
$\mathbf{5}^{2+\,b}$	−5.31	+3.57	−0.51	+90.9	+29.7	+1.8		+734.0
$\mathbf{6}^{2+\,c}$	−8.67	+1.83		+128.6	+11.4		−22.4	852.2

[a] In CD_2Cl_2 at 25 °C, see Schemes 1 and 2 for atom-labeling legend. [b] vs **5**. [c] vs **6**.

$Mn(CO)_3$ has very little effect on the ^{13}C *chemical* shift of the carbonyl groups (e.g., compare the ^{13}C NMR spectra of **3**, **4**, and **6** reported herein), substantial ^{13}C *paramagnetic* shifts observed for the carbonyl carbon nuclei in $\mathbf{6}^+$ and $\mathbf{6}^{2+}$ are noteworthy (Table 6). The magnitudes of these paramagnetic shifts are also consistent with "through-bond" rather than "through-space" interactions between the CO groups and the chromium centers in $\mathbf{6}^+$ and $\mathbf{6}^{2+}$.

For benzenoid π-systems, unpaired spin in the p orbital of an aromatic carbon atom polarizes (unpairs) electrons of the corresponding C(sp^2)−H σ-bond via an atomic exchange coupling mechanism.[54] This leads to paramagnetic shifts of the ^{13}C and the corresponding ^{1}H resonances occurring in opposite directions in the absence of substantial pseudo-contact interactions. Also, the unpaired spin signs and, hence, contact shifts alternate throughout benzenoid aromatic frameworks.[54] Figure 10 summarizes directions of the paramagnetic shifts observed for the ^{1}H, ^{13}C, and ^{14}N nuclei in $\mathbf{5}^z$ and $\mathbf{6}^z$ (z = 1+, 2+). Surprisingly, the 3,4-^{13}C nuclei of the *nonbenzenoid* C_5H_4 rings in $\mathbf{5}^z$ and $\mathbf{6}^z$ (z = 1+, 2+) undergo downfield paramagnetic shifts, which is in conflict with negative unpaired spin density in the p orbitals of these carbon atoms predicted from the ^{1}H NMR spectra of the complexes. This discrepancy might be due to the fact that the ^{13}C paramagnetic shift of a carbon atom within an aromatic scaffold depends not only on the unpaired spin density in its p orbital (which has zero coefficient at the nucleus) but also on spin densities at the neighboring carbon nuclei.[54] Such an explanation is supported by the observation that the resonances for carbon atoms at the junctions of five- and seven-membered rings in $[Cr(CN^2Az)_6]^+$ (^{2}Az = 2-azulenyl), which are analogous to the 3,4-C atoms in $\mathbf{5}^+$ and $\mathbf{6}^+$, *do* exhibit upfield paramagnetic shifts, as expected (Figure 10).[50,56]

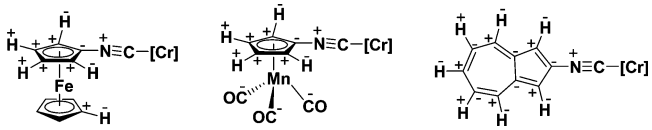

Figure 10. Observed directions of the ^{1}H, ^{13}C, and ^{14}N paramagnetic shifts for the nuclei in $[Cr(CNFc)_6]^{+/2+}$ (left), $[Cr(CNCm)_6]^{+/2+}$ (center), and $[Cr(CN^2Az)_6]^+$ (right). The symbols "−" and "+" denote upfield and downfield shifts, respectively, relative to chemical shifts of the nuclei in the corresponding diamagnetic zerovalent $Cr(CNR)_6$ or free CNR.

The presence of unpaired spin in the π-system of the aromatic substituent of a coordinated ligand is not necessarily evidence for metal−ligand π-covalency.[54,57,58] Nevertheless, we have recently demonstrated through DFT studies that M(dπ)→L(pπ*) back-bonding is indeed an important contributor to the mechanism of unpaired spin delocalization in binary isocyanide complexes of Cr(I).[13] Because of correlation effects, ligand-to-metal σ-interaction would favor placing excess negative spin on the ligating isocyanide carbon atoms in $\mathbf{5}^z$ and $\mathbf{6}^z$ (z = 1+, 2+).[41] The unpaired spin generated in this fashion may enter the π-system of the ligands via the atomic exchange coupling process (vide supra) operating in reverse. A similar mechanism was originally proposed by Drago and Fitzgerald,[58a] who doubted that unpaired spin density in the π-systems of the aryl substituents in $[Ni(NCPh)_6]^{2+}$ was a consequence of nickel−benzonitrile π-bonding.[59] Thus, one has to be cautious invoking metal−ligand π-covalency to explain the NMR patterns obtained for complexes $\mathbf{5}^{2+}$ and $\mathbf{6}^{2+}$, which exhibit only marginal M(dπ)→L(pπ*) interactions at best.

Concluding Remarks

Efficient syntheses of isocyanoferrocene and isocyanocymantrene from readily available starting materials have been established. These compounds represent an emerging new class[12,13] of aromatic isocyanides incorporating nonbenzenoid π-systems. The physical, chemical, electrochemical, and spectroscopic properties of the structurally characterized series $[Cr(CNFc)_6]^{0,1+,2+}$ indicate that the electronic influence of the ferrocenyl moiety, often considered to be similar to an alkyl group, is more similar to that of aryl substituents. Consequently, the donor/acceptor characteristics of the CNFc ligand are close to those of aryl isocyanides but quite different from those of alkyl isocyanides, including CNMe. In addition, we demonstrated that electronic properties (especially π-acidity) of the isocyanocyclopentadienide ligand can be tuned to a substantial extent by varying the nature of the metal fragment bound to its ring. Redox chemistry of $[Cr(CNFc)_6]^z$ (z > 2), carbonyl substitution transformations of $[Cr(CNCm)_6]^z$ (z = 0, 1+, 2+), and chemistry of other hitherto unknown organometallic isocyanocyclopentadienides are

(56) Robinson, R. E.; Holovics, T. C.; Deplazes, S. F.; Barybin, M. V. Manuscript in preparation.
(57) Drago, R. S. *Physical Methods in Chemistry*; Surfside Scientific Publishers: Gainesville, FL, 1992; Chapter 12.
(58) (a) Fitzgerald, R. J.; Drago, R. S. *J. Am. Chem. Soc.* **1967**, *89*, 2879−2883. (b) La Mar, G. N.; Sherman, E. O.; Fuchs, G. A. *J. Coord. Chem.* **1972**, *1*, 289−296.
(59) Kluiber, R. W.; Horrocks, W. D., Jr. *Inorg. Chem.* **1966**, *5*, 152−154.

currently under investigation and will be reported in due course.

Acknowledgment. Financial support of this work was provided by Kansas NSF EPSCoR, Kansas Technology Enterprise Corporation, and the University of Kansas. M.V.B. is grateful to KU Center for Research for the New Faculty GRF Award and to Professor David R. Benson for fruitful discussions and suggestions during manuscript preparation.

Supporting Information Available: Complete tables of atomic coordinates, bond distances, angles, and anisotropic displacement parameters for **5**·CH_2Cl_2, **6**, $\mathbf{5}^+[V(CO)_6]\cdot CH_2Cl_2$, and $\mathbf{5}^{2+}[BF_4]_2\cdot CH_2Cl_2$; cyclic voltammogram of $[Et_4N][V(CO)_6]$; ^1H, ^{13}C, and 2D NMR spectra of $[Cr(CN^2Az)_6][BF_4]$. This material is available free of charge via the Internet at http://pubs.acs.org.

OM049842N